



UDC 616-008.811.9:616-091.8:616-008.811.9:636.09  
DOI: 10.31548/ujvs.13(4).2022.60-74

## Cytomorphological characteristics of necroptates of internal organs of dogs in the early post-mortem period in the aspect of forensic veterinary examination

Ivan Yatsenko<sup>1\*</sup>, Roman Kazantsev<sup>2</sup>

<sup>1</sup>Full Doctor in Veterinary Sciences, Professor. ORCID: <https://orcid.org/0000-0001-8903-2129>.  
Institute of Veterinary Medicine and Animal Husbandry,  
62341, 1 Akademichna Str., v. Mala Danylivka, Kharkiv region, Ukraine

<sup>2</sup>Postgraduate Student. ORCID: <https://orcid.org/0000-0002-4479-1516>.  
Institute of Veterinary Medicine and Animal Husbandry,  
62341, 1 Akademichna Str., v. Mala Danylivka, Kharkiv region, Ukraine

**Abstract.** The relevance of the study lies in the need for forensic veterinary examination of animal corpses for scientific justification of informative diagnostic criteria for assessing the prescription of death, especially in the early post-mortem period. However, information about early post-mortem changes in dog cadavers at the microstructural level in the Ukrainian and foreign scientific literature is quite fragmentary. In this regard, the purpose of this paper is to establish the informative dynamics of the processes of cell destruction and bacterial contamination of internal organs of dog corpses during the first post-mortem day to establish probable expert criteria for the prescription of death of sub-expert animals during the forensic veterinary examination. A leading approach to the investigation of this problem is the method of obtaining a series of necroptates from lungs, heart, liver, spleen, kidney, pancreas, and brain from canine cadavers, over the same time interval during the first day after death. In cytological preparations obtained from necroptates, the number of destroyed cells and bacterial units was counted using optical microscopy. Based on the results of the dynamics of bacterial contamination and the intensity of morphological changes in spleen and pancreatic cells, their expert information content was established to solve the question of the prescription of death of dogs, regardless of weight and fatness indicators. It was found that the dynamics of bacterial contamination and cellular destruction of the brain, kidneys, and lungs of dog corpses have average expert information content, while the liver and heart are not informative. It was proved that the dynamics of destructive post-mortem processes in the cells of the compact organs of the corpses of dogs of different weight and fatness at the appropriate times probably do not differ and develop with the same intensity. The obtained results of the study will have significance both in the theory of forensic veterinary examination and directly applied, specifically when the forensic expert solves the question regarding the time limit for the death of the animal

**Keywords:** subexpert animals, cadaveric biotransformation, cell destruction, bacterial contamination, post-mortem organ changes

### Suggested Citation:

Yatsenko, I., & Kazantsev, R. (2022). Cytomorphological characteristics of necroptates of internal organs of dogs in the early post-mortem period in the aspect of forensic veterinary examination. *Ukrainian Journal of Veterinary Sciences*, 13(4), 60-74.

\*Corresponding author

## Introduction

Forensic veterinary examination is a new type of forensic examination in Ukraine, which was established in 2019 at the initiative of the National Research Centre “Ex. Prof. M.S. Bokarius Institute of Forensic Examinations” in the system of specialized state institutions of the Ministry of Justice of Ukraine (Klyuyev, 2019).

During a forensic veterinary examination, only a forensic veterinary expert is the subject of expert activity, who is authorized by law to resolve issues related to the identification and assessment of bodily injuries caused to an animal as a result of cruel treatment (Yatsenko & Parilovskyi, 2020; Randour *et al.*, 2021), during a traffic accident (Conroy *et al.*, 2019), poaching (Franckenberg *et al.*, 2015), in case of violation of their exploitation regime (Hall *et al.*, 2020), use in various spectacular events (Doelling *et al.*, 2021) etc. One of the objects of forensic veterinary examination is the cadaver of an animal (Ang *et al.*, 2019; Yatsenko & Kazantsev, 2021), examining which the forensic expert has to solve various questions, including regarding the time of its death (Yatsenko *et al.*, 2019).

Modern practice and tactics of forensic veterinary diagnostics in Ukraine require scientific substantiation of informative diagnostic criteria at the level of European forensic veterinary science (Parry & Stoll, 2020), namely regarding the assessment of the age of death of animals, primarily in the early post-mortem (antemortem) period. This is especially important for the most correct and precise establishment of the post-mortem interval and can substantially affect the further course of the investigation of crimes against animal life and health (Listos *et al.*, 2018).

The problem of determining the statute of limitations for the occurrence of animal deaths stays relevant for forensic veterinary experts, law enforcement agencies, and the court, which has been repeatedly discussed at scientific forums of various levels both in Ukraine and abroad (Munro *et al.*, 2020).

Currently, the most accessible method of determining the statute of limitations for the occurrence of animal death in forensic veterinary examination is a visual assessment of post-mortem changes, which are a macroscopic manifestation of biochemical and biophysical processes occurring in the animal's body after death. These include studies of cadaver spots, cooling, desiccation, post-mortem rigidity, supravital reactions, etc. They are quite informative, have important diagnostic forensic value, but do not always allow reliably and reasonably accurately establishing the duration of the post-mortem period of an animal corpse. This is explained by the fact that the natural changes that occur in the animal's body after death are complex and mostly unpredictable, since the emergence and development of post-mortem phenomena is influenced by a considerable range of factors (Tourou & Fitch, 2016).

The accuracy of visual methods for investigating an animal's corpse requires improvement. Therefore, the focus of forensic veterinary experts is shifted towards cytological and biochemical methods, which are based on systematic pathophysiological changes and are more precise and objective compared to such external factors.

At the current stage of the development of forensic veterinary expertise, scientists have developed and implemented into expert practice differential diagnostic criteria for determining the age of death of animals based on a limited range of signs (Listos *et al.*, 2018; Cao *et al.*, 2021). However, in forensic humane medicine, there are already many proven methods that give positive results and help in obtaining answers to numerous questions that have not yet been resolved. However, even the proposed latest research methods cause obstacles in their adaptation to forensic practice due to problems of material and technological support.

One of the options for solving this problem is to increase the accuracy and objectification of the structural and functional changes in the internal organs of the animal body of different morphological types in the post-mortem period (Ceciliason *et al.*, 2021).

A prominent place in forensic and veterinary thanatology is occupied by cytomorphological studies, the results of which can be used to establish the time of death of animals (Wunsche *et al.*, 2016). These issues are periodically discussed on the pages of scientific periodicals of Ukraine (Kazantsev & Yatsenko, 2021). However, many issues are still unresolved, including the cytomorphological characteristics of necroptates of internal organs of dogs in the early post-mortem period in the aspect of forensic veterinary examination. Thus, the issue under study is relevant from the standpoint of the practice of forensic veterinary expertise.

Therefore, the purpose of this study was to provide cytomorphological characteristics of necroptates of internal organs of dog cadavers in the early post-mortem period and to substantiate its informativeness for establishing the time of death during a forensic veterinary examination. Such studies were conducted in Ukraine for the first time.

## Literature Review

The possibilities of the classic method of examining animal cadavers – forensic autopsy, due to the frequent absence of macroscopic changes in the antemortem and early post-mortem period, are limited. This predetermines the need for forensic experts to use the latest research methods. Thus, Heng *et al.* (2009) described serial post-mortem radiographic data of the abdominal cavity in cadavers of dogs; Listos *et al.* (2016) provided a post-mortem estimate of time of death based on renal versus rectal temperature measurement; Panasiuk-Flak *et al.* (2021) proved the informativeness of the method of determining the time of death of dogs using atropine and pilocarpine in the early post-mortem period; Listos *et al.* (2017) demonstrated the possibility of estimating the time of death of animals by the development of microflora in the calf muscle of a dog; Li *et al.* (2020) provided molecular characterization of intestinal microbial shift in rats after death for 30 days; Paltian *et al.* (2019) described a procedure for estimating the post-mortem interval by determining the activities of catalase and delta-aminolevulinic acid dehydratase in liver, kidney, skeletal muscle, and brain tissues of mice; Swiss *et al.* (2022) investigated post-mortem changes in the electrical conductivity

of *Dicentrarchus labrax* skeletal muscles to estimate the post-mortem period; Dell'Annunziata *et al.* (2022) characterized the post-mortem interval using MALDI-TOF mass spectrometry analysis in mouse cadavers; El-Din *et al.* (2021) assessed post-mortem skin changes on animal and human cadavers to estimate time since death; Welson *et al.* (2021) determined the duration of death in male albino rats by investigating markers of oxidative stress, histopathological and molecular changes in internal organs; Zhang *et al.* (2022) established the statute of limitations for the occurrence of death of rats in the case of drowning by the composition of vitreous metabolites; Grell *et al.* (2018) substantiated the possibility of using imaging methods of sectional research in forensic veterinary medicine.

However, these and other proposed methods for determining the post-mortem interval require the use of appropriate equipment, special skills of forensic experts who use them, which is not always possible in everyday forensic veterinary practice.

A separate place in the diagnostic process is occupied by the analysis of microstructural (histological and cytological) changes in the internal organs of the animal corpse, which are a reflection of the biochemical and biophysical processes occurring in it after death, especially in the early post-mortem period, when its morphological changes are still invisible to the naked eye (Brooks Brownlie & Munro, 2016).

However, fragmentary studies of foreign scientists on histological changes in the internal organs and skeletal muscles of animal corpses of various species in the early post-mortem period do not cover the issue sufficiently.

Thus, the clarification of cytomorphological changes in the internal organs of dog corpses in the early post-mortem period in the practice of forensic veterinary expertise will be important both in the theory of forensic veterinary expertise, and directly applied, specifically when a forensic expert decides on the statute of limitations for the occurrence of death of a sub-expert animal.

## Materials and Methods

The study was conducted during 2021-2022 in the conditions of the Department of Sanitation, Hygiene, and Forensic Veterinary Medicine of the State Biotechnological University (Kharkiv).

For a randomized study, cadavers of domestic dogs (*Canis familiaris*,  $n = 14$ ) of the same age (3-4 years) were selected and divided into two experimental groups according to the principle of analogues in terms of their weight, degree of fattening, and in the absence of *anamnesis morbi*. All cadavers, according to the Law of Ukraine "About by-products of animal origin, not intended for human consumption" (Law of Ukraine No. 1089-IX..., 2020), are classified as category III by-products, safe for humans and other animals.

Group 1 included cadavers of dogs ( $n = 7$ ) with a weight of  $8.0 \pm 1.0$  kg, fatness above average. Other cadavers of dogs ( $n=7$ ) with below-average fatness and body weight of  $16.0 \pm 1.0$  kg were selected for Groups 2. After the same time interval (3 hours) during the first day after death, a

series of necroptates from the lungs, heart, liver, spleen, kidneys, pancreas, and brain in the size of  $1 \times 1 \times 1$  cm<sup>3</sup> were taken from the corpses of dogs of both groups. The study was conducted on the cadavers of dogs during the first day after the animal death before the emergence of late cadaveric phenomena, i.e., in the early post-mortem period. Native smears-imprints were made from each necroptate. The slides without prior fixation were immediately dried in air at 20°C. The obtained cytological preparations were stained according to the Pappenheim method in the A.I. Kryukov's modification, which provides the possibility of accelerated differentiation of structural elements of internal organs and their changes in smears-imprints at the cellular level (Zaporozhan *et al.*, 2002).

Microscopic examination of the obtained cytological preparations was performed using an optical binocular microscope Granum R50 (China) in the fields of view of  $10 \times 10$  and  $10 \times 100$ . Cytograms were obtained using a TouPCam UCMOS03100KPA digital camera (China), which were analysed at the final stage of the experiment, considering the recommendations of Ressel (2017).

In cytological preparations, the number of destructively changed cells and bacteria was counted separately in ten fields of view of the microscope, and then their average was determined.

The obtained digital data was statistically processed using a personal computer, using the software package "MS Office Excel 2016 (Statistica)", by calculating the arithmetic mean ( $M \pm m$ ) for each of the two indicators. The results of the study were evaluated by the level of significance ( $P$ ). The dynamics and intensity of cell destruction and bacterial contamination of the internal organs of dog cadavers in each group were compared for the previous and subsequent time intervals, as well as between each other in the intervals when they were first detected and at 24 hours of the experiment.

## Results and Discussion

The cytoarchitectonics of smears-imprints obtained from the tissues of the internal organs of dog cadavers, immediately after the onset of their death, preserves the usual lifetime condition. Thus, pneumocytes, cells of the ciliated epithelium, and neutrophils are well visualized on the cytograms of the lungs of the cadavers of dogs of both experimental groups. Nuclear cells present in large numbers are mainly well-differentiated respiratory epithelial cells. Pneumocytes (Fig. 1) and neutrophils (Fig. 1) are located discretely or in small clusters. They are spherical or oval. Their cytoplasm is grey, with a few optically transparent vacuoles. The cell nucleus contains compact chromatin, and the nucleolus is visualized in individual cells. The background of the cytogram is represented by a population of unchanged neutrophils. Ciliated epithelium of the lungs (Fig. 2) the cadavers of dogs of the EG 2 are located in small clusters. The cytoarchitecture of its cells is bipolar: at the basal pole there is a single nucleus with fine-grained chromatin and a nucleolus without signs of morphological changes. Pink cilia are visible at the apical pole.

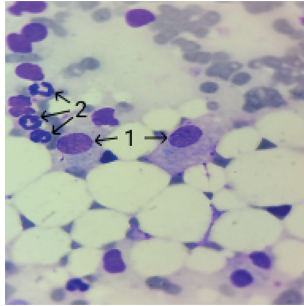


**Figure 1.** Cytochrome of the lungs of the corpse of a dog of the EG 1 immediately after death. Eyepiece 10×lens 100, stained according to Pappenheim-Kryukov  
*Note: 1 – pneumocytes; 2 – neutrophils*

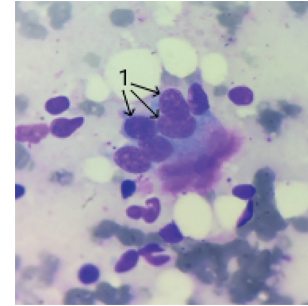


**Figure 1.** Cytochrome of the lungs of the cadaver of a dog of the EG 2 immediately after death. Eyepiece 10×lens 100, stained according to Pappenheim-Kryukov  
*Note: 1 – ciliated epithelium*

Brain cytochromes obtained immediately after the death of dogs of both research groups determine the average size of population cells: mainly neurons, oligodendrocytes, astrocytes. Neurons are large cells located singly. Their cytoplasm is blue with clear edges, without noticeable inclusions. The nucleus contains fine-grained chromatin and a single nucleolus.

The cytoarchitecture of neurons consists of a body (Fig. 3), from which an axon (Fig. 3) and a dendrite depart. The background of cytopreparations is represented

by diffusely located red blood cells. Astrocytes are medium-sized cells placed discretely. Their cytoplasm is light blue, without noticeable inclusions, contains a single nucleus with fine-grained chromatin without a nucleolus.

Oligodendrocytes are smaller cells located discretely. Their cytoplasm is light blue and contains a single nucleus with fine-grained chromatin without nucleoli. Inclusions are not visualized. The background of the cytopreparation is vacuolized, represented by ordinary neuropil and partially neuronal processes of the brain (Fig. 4), light pink or light purple.

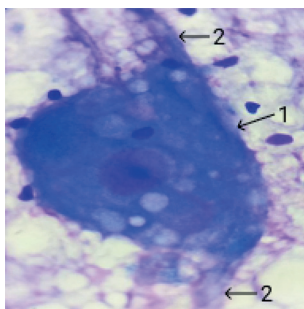


**Figure 3.** Cytochrome of the brain of the cadaver of a dog of the EG 1 immediately after death. Eyepiece 10×lens 100, stained according to Pappenheim-Kryukov  
*Note: 1 – the body of the neuron; 2 – the axons of the neuron*

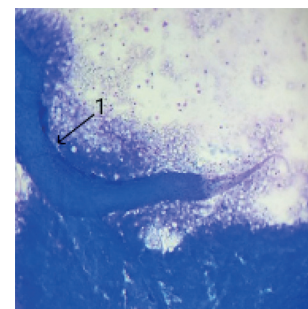


**Figure 4.** Cytochrome of the brain of the corpse of a dog of the EG 2 immediately after death. Eyepiece 10×lens 100, stained according to Pappenheim-Kryukov  
*Note: 1 – accumulation of neuronal processes*

Liver cytochromes obtained immediately after the death of dogs of both experimental groups reveal a dense population of hepatocytes of various shapes (Figs. 5, 6), mainly in

the form of spheres, with light blue granular cytoplasm, a large part of them contains a single nucleus with crystalline structures (Figs. 5; 6) and nucleoli with compact chromatin.

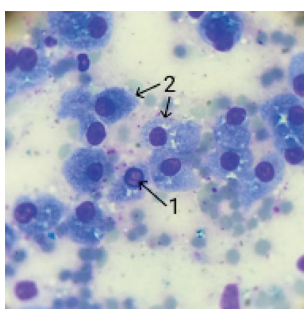


**Figure 5.** Cytochrome of the liver of the cadaver of a dog of EG 1 immediately after death. Eyepiece 10×lens 100, stained according to Pappenheim-Kryukov  
*Note: 1 – crystal structures in the nucleus of a hepatocyte; 2 – hepatocytes*

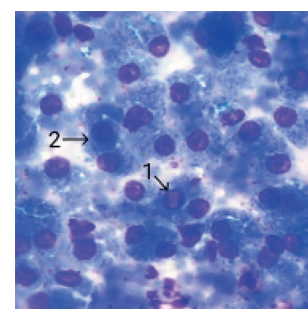


**Figure 6.** Cytochrome of the liver of the cadaver of a dog of EG 2 immediately after death. Eyepiece 10×lens 100, stained according to Pappenheim-Kryukov  
*Note: 1 – crystal structures in the nucleus of a hepatocyte; 2 – hepatocytes*

Liver cytograms obtained from the cadavers of dogs of both experimental groups 3 hours after death do not substantially differ in morphological changes in hepatocytes (Figs. 7, 8) from the structure of necroptates for the previous

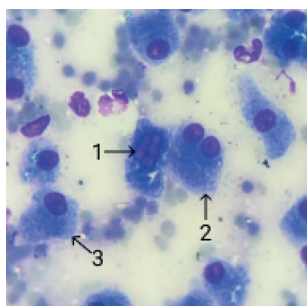


**Figure 7.** Cytogram of the liver of the corpse of a dog of the EG 1, 3 hours after death. Eyepiece 10×lens 100, stained according to Pappenheim-Kryukov  
**Note:** 1 – crystal structures in the nucleus of a hepatocyte; 2 – binuclear hepatocytes; 3 – hepatocyte

On the examination micropreparation of the liver obtained from the cadaver of a dog from the EG 2, a background represented by white blood cells of a small diameter is visualized (Fig. 9). However, pancreatocytes and erythrocytes

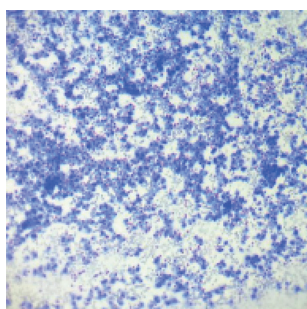


**Figure 9.** Cytogram of the liver of a dog cadaver of the EG 2, total cytogram 3 hours after death. Eyepiece 10×lens 10, stained according to Pappenheim-Kryukov

Cells of the pancreas of cadavers of dogs of both experimental groups are mainly represented by the epithelium of exocrine ducts (Fig. 11) both in clusters without clear cytoarchitecture and in structured formations in the form of clusters of acinar and tubular forms (Fig. 11). The

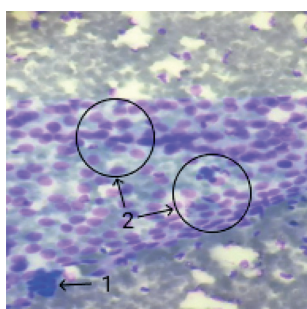


**Figure 11.** Cytogram of the pancreas of the cadaver of a dog of the EG 1, 3 hours after death. Eyepiece 10×lens 100, stained according to Pappenheim-Kryukov  
**Note:** 1 – accumulation of exocrine epithelium; 2 – accumulation of exocrine epithelium in the form of tubular structures

study period. There are binuclear cells of the liver parenchyma (Fig. 7) of various stages of mitosis. Hepatocyte nuclei often contain separate crystal structures (Figs. 7, 8), which is common in the cytoarchitecture of liver cells in dogs of this age.

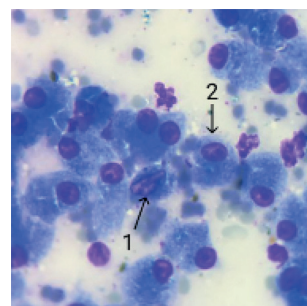


**Figure 8.** Cytogram of the liver of the corpse of a dog of the EG 2, 3 hours after death. Eyepiece 10×lens 100, stained according to Pappenheim-Kryukov  
**Note:** 1 – crystal structures in the nucleus of the hepatocyte; 2 – hepatocyte

of high density are observed on the examination micropreparation of the pancreas of the cadaver of a dog from the EG 1 (Fig. 10).

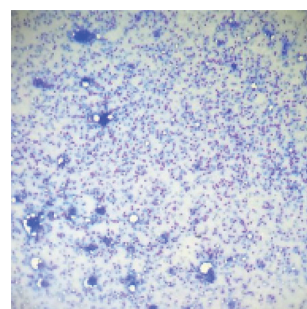


**Figure 10.** Cytogram of the pancreas of the corpse of a dog of the EG 1, total cytogram 3 hours after death. Eyepiece 10×lens 10, stained according to Pappenheim-Kryukov

cells are polygonal, with a large volume of cytoplasm, dark blue, and with a small nucleus. Cytograms of the pancreas of the cadaver of a dog from the EG 1 show a cluster of stromal cells (Fig. 12) around the exocrine epithelium (Fig. 12) against a light blue background.

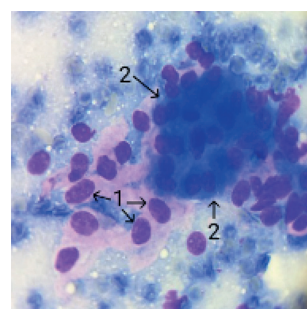


**Figure 12.** Cytogram of the pancreas of the cadaver of a dog of the EG 1, 3 hours after death. Eyepiece 10×lens 100, stained according to Pappenheim-Kryukov  
**Note:** 1 – stromal cells; 2 – exocrine epithelial cells

Acinar clusters of pancreatic cells (Fig. 13) of the cadaver of a dog of EG 2, 3 hours after death, polygonal with an eccentrically located round nucleus in each cell and two small nucleoli. Cytoplasm of exocrine epithelial cells in the form of a tubular

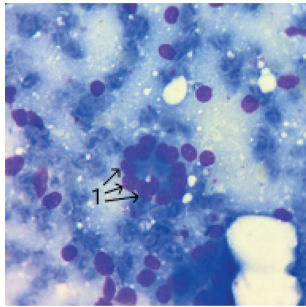


**Figure 13.** Cytogram of the pancreas of the cadaver of a dog of the EG 2, 3 hours after death. Eyepiece 10×lens 100, stained according to Pappenheim-Kryukov  
*Note: 1 – accumulation of exocrine epithelial cells in the form of an acinar structure*

Cytograms obtained from smears-imprints of the kidneys of the cadavers of dogs of the EG 1, 6 hours after death contain, in large quantities, erythrocytes and renal epithelium of nephrons (Fig. 15). However, there are no cells with signs of structural degeneration. Examining the cytograms of the kidneys obtained from the cadavers of dogs of the EG 2, it was observed that the cells are mainly located discretely and in tubular clusters of renal epitheliocytes of nephrons (Fig. 16). The cytoplasm of kidney epithelial

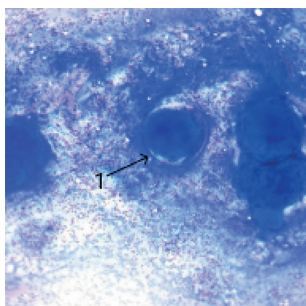


**Figure 15.** Cytogram of the kidney of the corpse of a dog of the EG 1, 6 hours after death. Eyepiece 10 × lens 10, stained according to Pappenheim-Kryukov  
*Note: 1 – renal body*

The cells of cytograms of the heart, obtained from the cadavers of dogs of the EG 1, 6 hours after death, are represented by

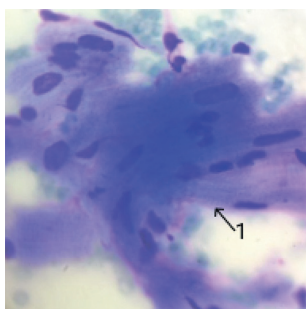


**Figure 17.** Cytogram of the heart of a cadaver dog of EG 1, 6 hours after death. Eyepiece 10×lens 100, stained according to Pappenheim-Kryukov  
*Note: 1 – cardiomyocytes*

structure (Fig. 14) occupies most of the area of each cell. The nuclei of individual pancreatic cells are basilar, uniform in structure, their shape is mainly spherical – from rounded to oval. Nuclear chromatin is speckled, with one small nucleoli with clear edges.

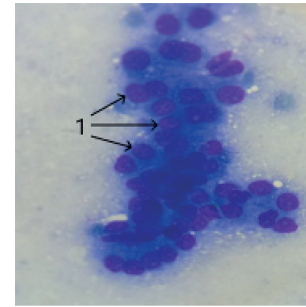


**Figure 14.** Cytogram of the pancreas of the cadaver of a dog of the EG 2, 3 hours after death. Eyepiece 10×lens 100, stained according to Pappenheim-Kryukov  
*Note: 1 – exocrine epithelial cells in the form of a tubular structure*

cells occupies half the cell area, most of them do not have a clear border between the cytoplasmic organelles. The colour of the cytoplasm varies from light blue to light pink. One nucleus with fine-grained chromatin is differentiated, and the nucleolus is not visible in it. Common features of the cytograms of the kidneys of cadavers of dogs of both experimental groups are numerous renal corpuscles and a protein-lipid, grey body that contains single unchanged neutrophils.

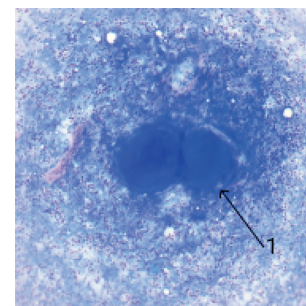


**Figure 16.** Cytogram of the kidney of the corpse of a dog of the EG 2, 6 hours after death. Eyepiece 10 × lens 10, stained according to Pappenheim-Kryukov  
*Note: 1 – renal body*

fragmented cardiomyocytes (Fig. 17) in clusters. Their cytoplasm is dark blue with well-defined transverse striations (Fig. 18).

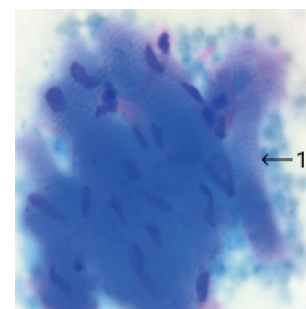


**Figure 18.** Cytogram of the heart of a cadaver dog of EG 1, 6 hours after death. Eyepiece 10×lens 100, stained according to Pappenheim-Kryukov  
*Note: 1 – cardiomyocytes*

Micropicture of cytograms obtained from the heart of cadavers of dogs of the EG 2, 6 hours after their death is characterized by a sparse cellular composition. The nuclei of cardiomyocytes (Fig. 19) are located parallel to the

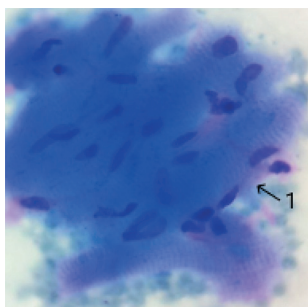


**Figure 19.** Cytogram of the heart of the cadaver of a dog of the EG 2, 6 hours after death. Eyepiece 10×lens 100, stained according to Pappenheim-Kryukov  
**Note:** 1 – cardiomyocytes

central axis of the cell, oval, without visible nucleoli. The background of cytopreparations is represented by red and white blood cells: red blood cells, neutrophils, small lymphocytes, and eosinophils (Fig. 20).

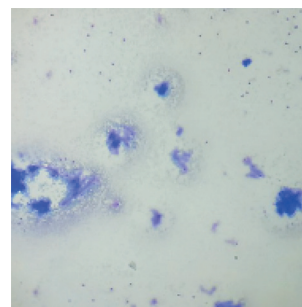


**Figure 20.** Cytogram of the heart of the cadaver of a dog of the EG 2, total cytogram 6 hours after death. Eyepiece 10 × lens 10, stained according to Pappenheim-Kryukov

Microscopic examination of smears-imprints of the spleen, obtained from the cadavers of dogs of the EG 1, 6 hours after their death, confirmed the presence of a heterogeneous population of white blood cells: lymphocytes of different sizes (Fig. 21), large lymphocytes (4%), small lymphocytes (79%), medium lymphocytes (11%), neutrophils (2%), eosinophils (1%), plasma cells (3%) (Fig. 21). No signs of cellular degeneration were recorded. However, when examining

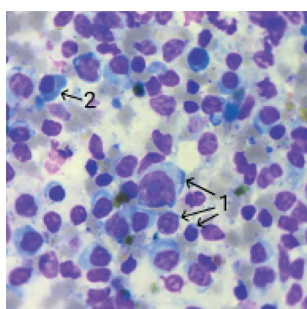


**Figure 21.** Cytogram of the spleen of the corpse of a dog of the EG 1, 6 hours after death. Eyepiece 10×lens 100, stained according to Pappenheim-Kryukov  
**Note:** 1 – lymphocytes of varied sizes; 2 – plasmocid

the cytological preparations of the spleen of the cadavers of dogs of group 2, 9 hours after their death, destroyed parenchyma cells (Fig. 22) and cocci-like bacteria (Fig. 22) were revealed for the first time. The background of cytograms is protein, grey, represented by high-density erythrocytes.

At 9 hours after the death of the dogs of both experimental groups, bacteria (Fig. 23, 24) and destroyed neurocytes (Fig. 24) were first detected in the brain.

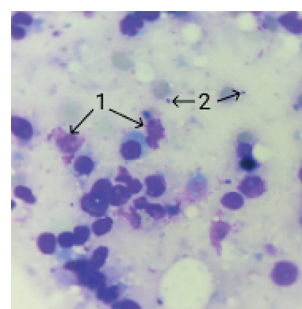


**Figure 22.** Cytogram of the spleen of the corpse of a dog of the EG 2, 9 hours after death. Eyepiece 10×lens 100, stained according to Pappenheim-Kryukov  
**Note:** 1 – destroyed cells; 2 – bacteria

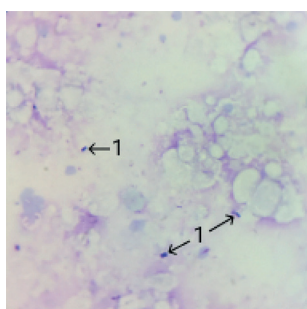


**Figure 23.** Cytogram of the brain of the cadaver of a dog of the EG 1, 9 hours after death. Eyepiece 10×lens 100, stained according to Pappenheim-Kryukov  
**Note:** 1 – bacteria

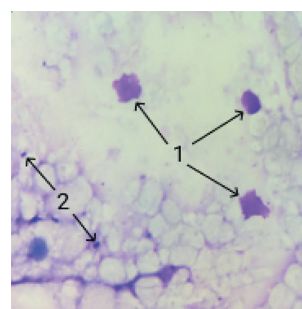


**Figure 24.** Cytogram of the brain of the corpse of a dog of the EG 2, 9 hours after death. Eyepiece 10 × lens 100, stained according to Pappenheim-Kryukov  
**Note:** 1 – destroyed cells; 2 – bacteria

The general cytogram of smears-prints of the myocardium of cadavers of dogs of both experimental groups is

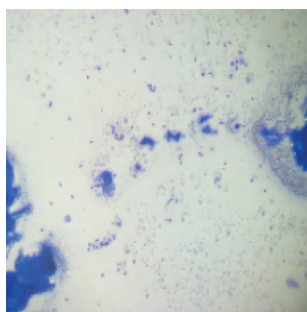


**Figure 25.** Cytogram of the heart of the cadaver of a dog of the EG 1, total cytogram 9 hours after death. Eyepiece 10×lens 10, stained according to Pappenheim-Kryukov

characterized by further fragmentation of cardiomyocytes (Fig. 25) with a violation of their striation (Fig. 26).

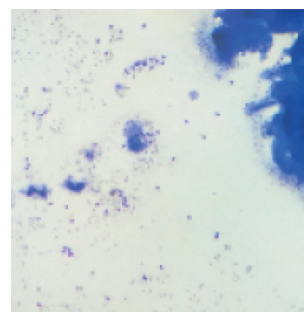


**Figure 26.** Cytogram of the heart of the cadaver of a dog of the EG 2, total cytogram 9 hours after death. Eyepiece 10×lens 10, stained according to Pappenheim-Kryukov

12 hours after the death of the dogs of both experimental groups, the number of bacteria in the brain increases. Bacteria are placed in clusters around neurocytes (Fig. 27).

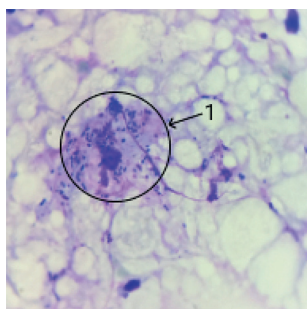


**Figure 27.** Cytogram of the brain of the cadaver of a dog of the EG 1, 12 hours after death. Eyepiece 10×lens 100, stained according to Pappenheim-Kryukov  
*Note:* 1 – accumulation of bacteria around the neuron body

They are cocci and rod-shaped (Fig. 28). Due to the vital activity of bacteria, the destruction of brain substance cells increases (Fig. 28).

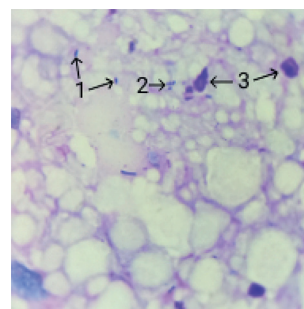


**Figure 28.** Cytogram of the brain of the cadaver of a dog of the EG 2, 12 hours after death. Eyepiece 10×lens 100, stained according to Pappenheim-Kryukov  
*Note:* 1 – cocci-like bacteria; 2 – rod-shaped bacteria; 3 – destroyed neurocytes

Intensive processes of cell destruction with simultaneous bacterial contamination were also observed in other internal organs. Thus, on the cytograms of the pancreas of the cadavers of dogs of EG 1, intensive bacterial

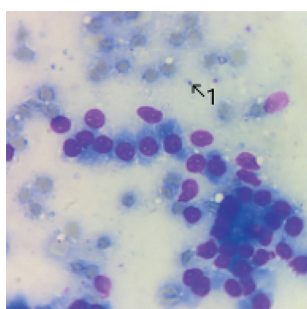


**Figure 29.** Cytogram of the pancreas of the corpse of a dog of the EG 1, 12 hours after death. Eyepiece 10×lens 100, stained according to Pappenheim-Kryukov  
*Note:* 1 – bacteria

colonization is noted (Fig. 29), and in the tissue of the spleen of cadavers of dogs of EG 2, apart from bacterial contamination (Fig. 30), significant destructive changes are detected (Fig. 30).

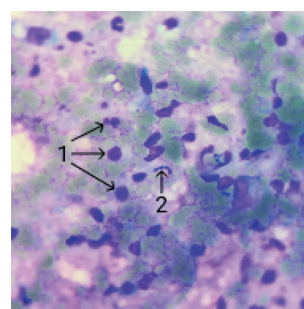


**Figure 30.** Cytogram of the spleen of the corpse of a dog of the EG 2, 12 hours after death. Eyepiece 10 × lens 100, stained according to Pappenheim-Kryukov  
*Note:* 1 – destroyed cells; 2 – bacteria

12 hours after death, it can be stated that on the cytograms of the liver obtained from the cadavers of dogs of both experimental groups, the processes of destruction

of the parenchyma cells of the organ continue to intensify (Figs. 31, 32), which occurs against the background of colonization by bacteria (Figs. 31, 32).



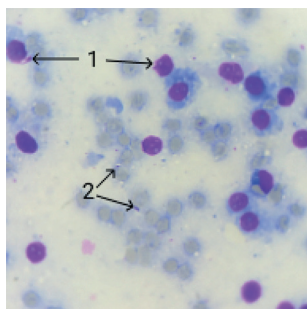


**Figure 31.** Cytochrome of the liver of the corpse of a dog of the EG 1, 12 hours after death. Eyepiece 10×lens 100, stained according to Pappenheim-Kryukov  
**Note:** 1 – destroyed cells; 2 – bacteria

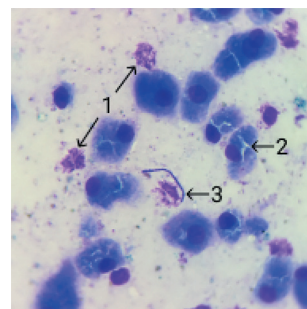


**Figure 32.** Cytochrome of the liver of the cadaver of a dog of the EG 1, 15 hours after death. Eyepiece 10×lens 100, stained according to Pappenheim-Kryukov  
**Note:** 1 – destroyed cells; 2 – hepatocyte; 3 – bacteria

On the cytochrome of the liver of the corpse of a dog of the EG 2, obtained 15 hours after its death, the destructive changes in the cells are noted (Fig. 33) and the number of bacteria (Fig. 33) do not differ significantly from the necrotates obtained in the previous periods of the study, except

for the presence in the nuclei of hepatocytes of non-specific crystal structures (Fig. 33), which is a variant of the cytological norm for these animals in adulthood. 18 hours after the death of dogs of the EG 1, the presence of bacterial colonies around the bodies of neurons in the brain was noted (Fig. 34).

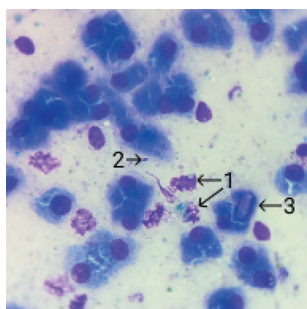


**Figure 33.** Cytochrome of the liver of the corpse of a dog of the EG 2, 15 hours after death. Eyepiece 10×lens 100, stained according to Pappenheim-Kryukov  
**Note:** 1 – destroyed cells; 2 – bacteria; 3 – crystal structure in the nucleus of the hepatocyte

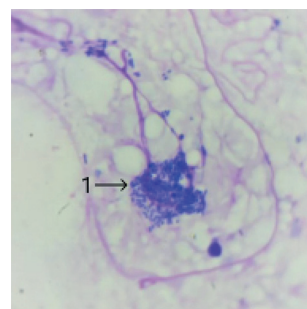


**Figure 34.** Cytochrome of the brain of the cadaver of a dog of the EG 1, 18 hours after death. Eyepiece 10×lens 100, stained according to Pappenheim-Kryukov  
**Note:** 1 – accumulation of bacteria around the neuron's body

However, 21 hours after the death of dogs, bacterial contamination of the brain substance is detected in both

experimental groups in the form of clusters of bacterial colonies (Figs. 35, 36) over the entire area of the object under study.

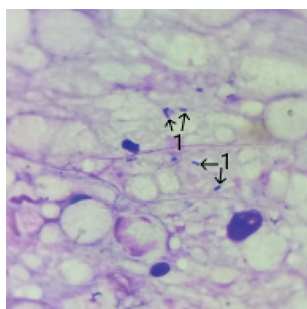


**Figure 35.** Cytochrome of the brain of the cadaver of a dog of the EG 1, 21 hours after death. Eyepiece 10×lens 100, stained according to Pappenheim-Kryukov  
**Note:** 1 – bacteria

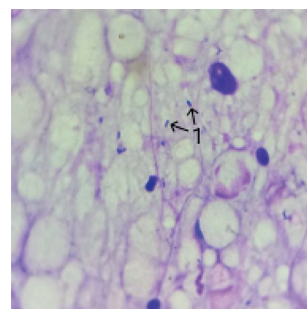


**Figure 36.** Cytochrome of the brain of the cadaver of a dog of the EG 2, 21 hours after death. Eyepiece 10×lens 100, stained according to Pappenheim-Kryukov  
**Note:** 1 – bacteria

24 hours after the death of dogs, active destructive processes are noted in their spleen. Thus, on the cytochrome of the spleens of the cadavers of dogs of both experimental groups, the prevalence of bacteria is observed (Figs. 37, 38)

with localization over the entire area of cytopreparations. Thus, on cytological preparations, the processes of total destruction in the cellular composition were recorded (Figs. 37; 38).

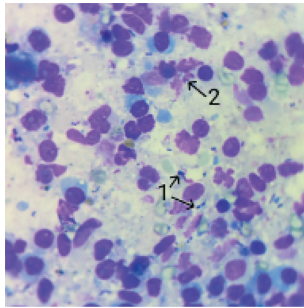


**Figure 37.** Cytogram of the spleen of the cadaver of a dog of the EG 1, 24 hours after death. Eyepiece 10×lens 100, stained according to Pappenheim-Kryukov  
**Note:** 1 – bacteria; 2 – destroyed cells

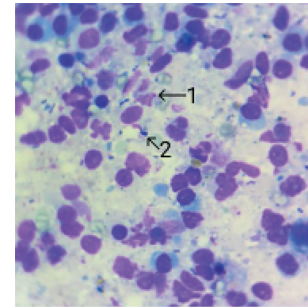


**Figure 38.** Cytogram of the spleen of the cadaver of a dog of the EG 2, 24 hours after death. Eyepiece 10×lens 100, stained according to Pappenheim-Kryukov  
**Note:** 1 – destroyed cells; 2 – bacteria

Attention is drawn to the cytological picture of the liver and heart, smears-prints from which were obtained a day after the death of animals. Necrobiotic processes in these internal organs are close to cytolysis. Only single indestructible hepatocytes are preserved on

liver cytograms of cadavers of dogs of the EG 1 (Fig. 39). However, most cells are subject to total destruction (Fig. 39). At the same time, cytograms of the heart of cadavers of dogs of the EG 1 reflect fragmentation of cardiomyocytes (Fig. 40).

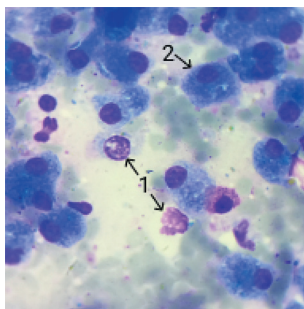


**Figure 39.** Cytogram of the liver of the cadaver of a dog of the EG 1, 24 hours after death. Eyepiece 10×lens 100, stained according to Pappenheim-Kryukov  
**Note:** 1 – destroyed cells; 2 – hepatocyte

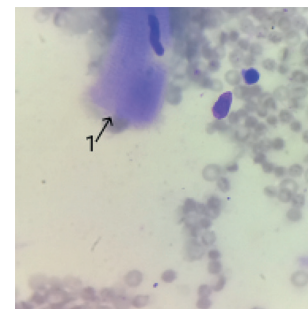


**Figure 40.** Cytogram of the heart of the cadaver of a dog of the EG 1, 24 hours after death. Eyepiece 10×lens 100, stained according to Pappenheim-Kryukov  
**Note:** 1 – cardiomyocyte

During the cytological examination of smears-prints of internal organs after 12 hours of the experiment, their common optical property of eosinophilic staining was established, which is evidently associated with the beginning of the destruction of nuclear components of cells, lysis by karyolium, the exit of nuclear components outside the

nucleus and their mixing with substance of the cytoplasm.

Observation of the quantitative dynamics of bacterial contamination of cadaver organs in dogs of both experimental groups at the same time intervals in the early post-mortem period allowed establishing that the intensity of its manifestation is specific for each of them (Table 1).

**Table 1.** Dynamics of bacterial contamination of internal organs of cadavers of dogs of experimental groups at the same time intervals of the early post-mortem period (n = 14)

Experiment interval (h)	Experimental group	Number of bacterial units on cytograms of internal organs						
		Lungs	Heart	Liver	Spleen	Kidneys	Pancreas	Brain
0-3	1	Bacterial contamination is not observed						
	2	Bacterial contamination is not observed						
3-6	1	–	–	–	1.36 ± 0.13	–	–	–
	2	–	–	–	1.83 ± 0.22	–	–	–
6-9	1	–	–	–	4.23 ± 0.06***	–	10.07 ± 0.11	1.01 ± 0.03
	2	–	–	–	4.51 ± 0.08***	–	11.83 ± 0.22***	1.34 ± 0.05**
9-12	1	0.94 ± 0.04	–	–	8.23 ± 0.07***	2.97 ± 0.08^	16.07 ± 0.09***	1.49 ± 0.08**
	2	1.11 ± 0.03*	–	–	8.21 ± 0.13***	2.60 ± 0.09	13.86 ± 0.08***	1.99 ± 0.05***
12-15	1	1.13 ± 0.03**	–	1.11 ± 0.03	16.33 ± 0.12***	3.8 ± 0.04***	16.70 ± 0.06***	2.41 ± 0.05***
	2	1.16 ± 0.04	–	1.07 ± 0.05	15.70 ± 0.26***	3.51 ± 0.04***	16.16 ± 0.05***	3.24 ± 0.06***
15-18	1	1.23 ± 0.05	–	2.10 ± 0.06***	19.69 ± 0.36***	4.43 ± 0.08***	17.79 ± 0.07***	2.97 ± 0.08**
	2	1.29 ± 0.03*	–	2.61 ± 0.06***	18.86 ± 0.17***	4.51 ± 0.04***	18.33 ± 0.04***	3.93 ± 0.05***

Table 1, Continued

Experiment interval (h)	Experimental group	Number of bacterial units on cytograms of internal organs						
		Lungs	Heart	Liver	Spleen	Kidneys	Pancreas	Brain
18-21	1	1.33 ± 0.04	–	3.11 ± 0.08 <sup>***</sup>	21.01 ± 0.21 <sup>**</sup>	4.99 ± 0.05 <sup>***</sup>	18.47 ± 0.04 <sup>***</sup>	3.29 ± 0.04 <sup>*</sup>
	2	1.37 ± 0.05	–	3.34 ± 0.07 <sup>***</sup>	20.07 ± 0.06 <sup>***</sup>	5.24 ± 0.06 <sup>***</sup>	18.71 ± 0.04 <sup>***</sup>	4.46 ± 0.06 <sup>***</sup>
21-24	1	1.50 ± 0.03 <sup>**</sup>	0.91 ± 0.05	3.97 ± 0.05 <sup>***</sup>	22.54 ± 0.05 <sup>***</sup>	6.86 ± 0.06 <sup>***</sup>	19.20 ± 0.11 <sup>***</sup>	4.43 ± 0.08 <sup>***</sup>
	2	1.50 ± 0.02 <sup>**</sup>	1.00 ± 0.05	4.26 ± 0.07 <sup>**</sup>	24.40 ± 0.22 <sup>***^</sup>	7.53 ± 0.06 <sup>***^</sup>	21.16 ± 0.39 <sup>***^</sup>	5.77 ± 0.06 <sup>***^</sup>

Note: \* $P < 0.05$ , \*\* $P < 0.01$ , \*\*\* $P < 0.001$  compared to the indicators of the previous study period within the experimental group; <sup>\*</sup> $P < 0.05$ , <sup>\*\*</sup> $P < 0.01$ , <sup>\*\*\*</sup> $P < 0.001$  compared to the indicators between the experimental groups in the same time frame of the experiment

It was established that 3 hours after the death of dogs in both experimental groups, bacteria were not detected in any organ (Table 1). However, as early as 6 hours of follow-up, they are registered in the spleen of cadavers of dogs of these groups. During the experimental period, the number of bacteria in the internal organs of the cadavers of dogs of the experimental groups gradually increases. Thus, at 24 hours, it significantly increases by 16.57 times ( $P < 0.001$ ) in the spleen of cadavers of dogs of the EG 1, and by 13.33 times ( $P < 0.001$ ) – in cadavers of animals of the EG 2 compared to the period of their first detection (at 6 hours of the experiment). By comparing the quantitative indicators of bacterial contamination on the spleen cytograms of cadavers of dogs of the experimental groups 1 and 2, it was found that at 6 hours of examination, these indicators did not significantly differ from each other. At the same time, at 24 hours, the number of bacteria in the spleen of cadavers of dogs of the EG 2 was significantly higher by 1.08 times ( $P < 0.001$ ) than in the spleen of cadavers of dogs of the EG 1.

The bacteria appeared in the pancreas and brain of cadavers of dogs in both experimental groups at 9 hours of examination. During the examination period, it was found that the number of bacteria gradually increased on the cytograms of the pancreas and brain of cadavers of dogs of the experimental groups 1 and 2.

Thus, at 24 hours, their number significantly increased by 1.9 times ( $P < 0.001$ ) in the pancreas of the cadavers of dogs of the EG 1 and by 1.79 times ( $P < 0.001$ ) – in the cadavers of animals of the EG 2 compared to the period when they were detected for the first time (at 9 hours of the experiment). Comparing the quantitative indicators of bacterial contamination on the cytograms of the pancreas of cadavers of dogs of the experimental groups 1 and 2 with each other, it was found that at 9 hours the number of bacteria in this organ of cadavers of dogs of the EG 2 significantly increased by 1.17 times ( $P < 0.001$ ), and at 24 hours – by 1.1 times ( $P < 0.01$ ) compared with such indicators in the EG 1.

An analogous trend was found when analysing brain cytograms in the cadavers of dogs of both experimental groups. Thus, at 24 hours of the experiment, the number of bacteria in the brain of cadavers of dogs of the EG 1 significantly increased by 4.39 times ( $P < 0.001$ ) and in cadavers of animals of the EG 2 – by 4.31 times ( $P < 0.001$ ) compared to the period when they were detected for the first time (at 9 hours of the experiment). Comparing the quantitative indicators of bacterial contamination on the brain cytograms of cadavers of dogs of experimental groups 1 and 2 with each other for 9 hours, it was found that the number of bacteria in this organ of cadavers of dogs of EG 2 significantly increased by 1.33 times ( $p < 0.01$ ) than in EG 1.

These dynamics persisted for 24 hours of the study. Thus, the number of bacteria in the brain of cadavers of dogs of EG 2 significantly increased by 1.3 times ( $P < 0.01$ ) compared to EG 1.

After 12 hours of the experiment, the bacteria were recorded simultaneously in the lungs and kidneys of cadavers of dogs of both experimental groups. During the study period, the number of bacteria in the lungs and kidneys of cadavers of dogs in these groups gradually increased with varying intensity over the examination time intervals.

Thus, at 24 hours, the number of bacteria in the lungs of cadavers of dogs of the EG 1 was significantly higher by 1.6 times ( $P < 0.01$ ) compared to the time when they were first detected. Comparing the indicators of bacterial contamination on the cytograms of the lungs of cadavers of dogs of experimental groups 1 and 2 with each other, it was found that by 12 hours, the number of bacteria in this organ of cadavers of dogs of EG 2 significantly increased by 1.18 times ( $P < 0.05$ ) compared to EG 1. However, at 24 hours of examination, the values of bacterial contamination indicators did not significantly differ.

A comparable dynamic of bacterial contamination was found in the kidneys of cadavers of dogs of both experimental groups. Thus, at 24 hours in the kidneys of cadavers of dogs of EG 1, the number of bacteria is significantly higher by 2.31 times ( $P < 0.001$ ), and in EG 2 – by 2.9 times ( $P < 0.001$ ) compared to the period when they are detected for the first time (at 12 hours of the experiment). Comparing the indicators of bacterial contamination on the kidney cytograms of cadavers of dogs of experimental groups 1 and 2 with each other, it was found that at 12 hours of observation, the number of bacteria in this organ of cadavers of dogs of EG 1 is significantly higher by 1.14 times ( $P < 0.05$ ), and at 24 hours – by 1.1 times ( $P < 0.001$ ) compared to EG 2.

According to the results of analysis of liver cytograms of cadavers of dogs of both experimental groups, it was found that bacteria in this organ appear for the first time at 15 hours of examination. Further, during the last study period, the number of bacteria in both groups gradually increases at certain examination time intervals. Thus, at 24 hours, the number of bacteria in the liver of cadavers of dogs of experimental groups 1 and 2 is significantly higher by 3.58 times ( $P < 0.001$ ) and 3.98 ( $P < 0.05$ ), respectively, compared to the period when they are detected for the first time (at 15 hours of the experiment). At the same time, at 24 hours, the number of bacteria in the liver of cadavers of dogs of EG 2 significantly increases by 1.07 times ( $P < 0.05$ ) compared to EG 1. At 15 hours of the experiment, there was no statistically significant difference in the number of bacteria on the liver cytograms of cadavers of dogs of experimental groups 1 and 2.

Late bacterial contamination is inherent in the myocardium. Bacteria on the cytograms of the heart of cadavers of dogs of both experimental groups were detected for the first time after death at 24 hours of the experiment. Comparing the indicators of contamination of the heart by bacteria in the cadavers of dogs of experimental 1 and 2 with each other, a

significant difference between these indicators has not been established. Analysing the quantitative dynamics of destructive cells in the organs of cadavers of dogs of both experimental groups at the same time intervals of the early post-mortem period, it was found that the intensity of their manifestation is specific for the organ in which they are detected (Table 2).

**Table 2.** Dynamics of destructive cells in the internal organs of dog cadavers at the same time intervals in the early post-mortem period (n = 14)

Experiment interval(h)	Experimental group	Number of units of destructive cells on cytograms of internal organs						
		Lungs	Heart	Liver	Spleen	Kidneys	Pancreas	Brain
0-3	1	No destructive cells were observed						
	2	No destructive cells were observed						
3-6	1	–	–	–	–	–	2.56 ± 0.26	–
	2	–	–	–	–	–	2.49 ± 0.12	–
6-9	1	–	–	–	9.73 ± 0.27	–	9.86 ± 0.10 <sup>***</sup>	0.87 ± 0.04
	2	–	–	–	10.76 ± 0.25 <sup>^</sup>	–	7.70 ± 0.08 <sup>***</sup>	0.94 ± 0.04
9-12	1	0.44 ± 0.06	–	–	14.87 ± 0.25 <sup>***</sup>	1.91 ± 0.06 <sup>^^</sup>	12.33 ± 0.14 <sup>***</sup>	1.16 ± 0.04 <sup>^^</sup>
	2	0.40 ± 0.04	–	–	16.53 ± 0.09 <sup>***</sup>	1.49 ± 0.08	11.53 ± 0.16 <sup>***</sup>	1.23 ± 0.05 <sup>^^</sup>
12-15	1	0.87 ± 0.04 <sup>^^</sup>	–	2.14 ± 0.10	22.37 ± 0.14 <sup>***</sup>	2.63 ± 0.04 <sup>***</sup>	13.16 ± 0.04 <sup>^^</sup>	1.67 ± 0.04 <sup>***</sup>
	2	1.01 ± 0.03 <sup>***</sup>	–	2.17 ± 0.04	18.59 ± 0.12 <sup>***</sup>	2.41 ± 0.05 <sup>***</sup>	12.61 ± 0.07 <sup>***</sup>	1.67 ± 0.05 <sup>***</sup>
15-18	1	1.36 ± 0.05 <sup>***</sup>	–	3.76 ± 0.08 <sup>***</sup>	23.40 ± 0.54	3.01 ± 0.03 <sup>***</sup>	13.53 ± 0.07 <sup>^^</sup>	3.21 ± 0.07 <sup>***</sup>
	2	1.34 ± 0.05 <sup>^^</sup>	–	3.64 ± 0.04 <sup>***</sup>	22.93 ± 0.06 <sup>***</sup>	2.97 ± 0.08 <sup>^^</sup>	13.53 ± 0.04 <sup>^^</sup>	3.71 ± 0.07 <sup>***</sup>
18-21	1	1.96 ± 0.06 <sup>***</sup>	–	5.26 ± 0.08 <sup>***</sup>	27.09 ± 0.55 <sup>^^</sup>	3.21 ± 0.03 <sup>***</sup>	14.24 ± 0.07 <sup>***</sup>	5.99 ± 0.03 <sup>***</sup>
	2	2.06 ± 0.06 <sup>***</sup>	–	5.50 ± 0.05 <sup>***</sup>	27.93 ± 0.41 <sup>***</sup>	3.29 ± 0.04 <sup>^</sup>	14.79 ± 0.04 <sup>***</sup>	5.54 ± 0.05 <sup>***</sup>
21-24	1	2.51 ± 0.03 <sup>***</sup>	–	8.50 ± 0.13 <sup>***</sup>	36.74 ± 0.43 <sup>***</sup>	4.06 ± 0.07 <sup>***</sup>	15.71 ± 0.10 <sup>***</sup>	6.71 ± 0.05 <sup>***</sup>
	2	2.49 ± 0.04 <sup>^^</sup>	–	8.94 ± 0.09 <sup>***</sup>	38.54 ± 0.16 <sup>***</sup>	4.43 ± 0.08 <sup>***</sup>	15.83 ± 0.08 <sup>***</sup>	6.46 ± 0.08 <sup>***</sup>

**Note:** <sup>\*</sup>P < 0.05, <sup>\*\*</sup>P < 0.01, <sup>\*\*\*</sup>P < 0.001 compared to the indicators of the previous study period within the experimental group; <sup>^</sup>P < 0.05, <sup>^^</sup>P < 0.01, <sup>^^^</sup>P < 0.001 compared to the indicators between the experimental groups in the same time frame of the experiment

It was established that 3 hours after the death of dogs of both experimental groups, destructive cells were not detected in any organ (Table 2). However, as early as 6 hours of the experiment, destructive cells are registered in the pancreas of cadavers of dogs of both experimental groups, although a statistically significant difference in their number has not been established.

During the study period, the number of destructively altered cells in the studied organs of dog cadavers gradually increases. Thus, at 24 hours, their number increases significantly by 6.14 times (P < 0.001) in the pancreas of cadavers of dogs of EG 1 and by 7.71 times (P < 0.001) – by EG 2 compared to the period when they are detected for the first time (at 6 hours of the experiment).

At 9 hours of the experiment, destructively altered cells were found in the spleen and brain of cadavers of dogs of both experimental groups. During the entire study period, the number of destructive cells in the spleen and brain of dog cadavers in both experimental groups gradually increased. Thus, at 24 hours of the experiment, their number in the spleen of cadavers of dogs of EG 1 significantly increases by 3.78 times (P < 0.001) and by 3.58 times (P < 0.001) – EG 2 compared to the period when they are detected for the first time (at 9 hours of the experiment). Comparing the number of destructive cells on the spleen cytograms of cadavers of dogs of experimental groups 1 and 2 with each other at 9 hours of the experiment, it was found that the number of destructive cells in this organ of cadavers of dogs of EG 2 is significantly greater by 1.14 times (P < 0.05) compared to that in EG 1. Similar dynamics

were found at 24 hours of the experiment, when the indicator of the number of destroyed cells in the spleen of cadavers of dogs of EG 2 significantly increased by 1.05 times (P < 0.01) compared to its values in EG 1.

During the analysis of brain cytograms of cadavers of dogs of both experimental groups, it was found that at 24 hours of the experiment, the number of destructive cells in this organ of cadavers of dogs of experimental groups 1 and 2 is significantly higher by 7.71 times (P < 0.001) and 6.87 times (P < 0.001), respectively, compared to the period when they are detected for the first time (at 9 hours of the experiment). There was no statistically significant difference in the number of destructive cells on the brain cytograms of the cadavers of dogs of experimental groups 1 and 2 at 9 hours of the experiment. However, at 24 hours of the experiment, the number of destructive cells in the brain of cadavers of dogs of EG 1 significantly increased by 1.04 times (P < 0.05) compared to that of cadavers of dogs of EG 2. The obtained data on the post-mortem cytomorphology of brain cells coincide with the results of the studies of Wunsche *et al.* (2016), who investigated the cytograms of the human brain to identify lifelong organic lesions of its membranes during septic processes.

After 12 hours of the experiment, destructive cells appear in the lungs and kidneys of cadavers of dogs of both experimental groups.

Thus, during the study of cytograms of the lungs of cadavers of dogs of experimental groups 1 and 2, it was found that the number of destructively altered cells significantly increases by 5.7 times (P < 0.001) and 6.23 times (P < 0.01),

respectively, compared to the period when they are detected for the first time (at 12 hours of the experiment). Comparing the number of destructive cells on the cytograms of the lungs of cadavers of dogs of experimental groups 1 and 2 at 15 and 24 hours of the experiment, no statistically significant difference was established.

In the kidneys of cadavers of dogs of EG 1, the number of destructive cells at 24 hours was significantly greater by 2.13 times ( $P < 0.001$ ) and 2.97 times ( $P < 0.001$ ), respectively, compared to the period when they were detected for the first time (at 12 hours of the experiment). At the same time, at 12 h of the experiment, the number of destructive cells in the kidneys of the cadavers of dogs of EG 1 is significantly 1.25 times greater ( $P < 0.01$ ) compared to those of cadavers of dogs of EG 2. However, at 24 hours, this indicator in the kidneys of cadavers of dogs of EG 2 significantly increased by 1.1 times ( $P < 0.05$ ) than in cadavers of dogs of EG 1.

Examining the cytograms of the livers of dog cadavers in both groups, it was established that destructive cells in this organ appear for the first time at 15 hours of observation and their number gradually increases during the experimental period. Thus, at 24 hours of the experiment, the number of destructive cells in the liver of the cadavers of dogs of experimental groups 1 and 2 probably increased by 3.97 times ( $P < 0.001$ ) and 4.11 times ( $P < 0.001$ ), respectively, compared to the time when they were first detected (at 15 hours of the experiment). At 24 hours of the experiment, the number of such cells in the liver of cadavers of dogs of EG 2 significantly increased by 1.05 times ( $P < 0.05$ ) than in cadavers of dogs of EG 1 (Table 2).

Comparing the number of destructive cells on liver cytograms of dog cadavers between experimental groups 1 and 2 at 15 hours of the experiment, no statistically significant difference was found. The obtained data completely coincide with the studies of Ceciliason *et al.* (2021), who established the sequence of processes of necrobiosis of liver cells in humans.

During the study of cytograms of the heart of cadavers of animals of both experimental groups, no destructive changes in cells were registered during the experimental period. The obtained data on the cytomorphology of the heart confirm the results of the studies of Welson *et al.* (2021), who prove that the processes of fragmentation and vacuolization of the cytoplasm in rat cardiomyocytes begin no earlier than 96 h after the death of the animals.

Thus, summarizing the results obtained during the cytomorphological study of the compact organs of dog corpses with different indicators of mass and fatness, the authors of this study believe that the most intense cadaveric dynamics of bacterial contamination and cell destruction in the first day of the post-mortem period occurs in the

spleen and pancreas. Therewith, pronounced putrefactive biotransformation of the spleen is caused by decomposition products in these organs. Necrobiotic changes that develop intensively in the cells of the spleen and pancreas evidently provoke bacterial contamination. At the same time, bacterial contamination of pancreatic cells, which was observed later than in the spleen, may also be the result of an inhibitory effect on the intensity of bacterial growth of autolytic enzymes of exocrine epithelial cells. Therefore, the intensity of dynamics of cytomorphological changes in spleen and pancreatic cells is of informative value when deciding on the duration of the post-mortem period during the first day after the death of dogs.

## Conclusions

Based on a randomized study of cells of compact organs of cadavers of dogs, it was proved that only cytomorphological changes in spleen and pancreas cells in terms of their intensity have expert information content to solve the question of the prescription of death during the first day of the post-mortem period in dogs, regardless of their body weight and fatness. The dynamics of bacterial contamination and destruction of brain, kidney, and lung cells are moderately informative, while the liver and heart are uninformative.

The most intense simultaneous dynamics of bacterial contamination and cell destruction occurs in the spleen and pancreas of dog cadavers, regardless of their body weight and fatness, which is evidently associated with autolysis of pancreacites, the release of a considerable number of proteolytic enzymes from their lysosomes. Simultaneous pronounced putrefactive biotransformation of the spleen is caused by the emergence of a considerable number of protein catabolism products. Necrobiotic changes that dynamically develop in the cells of the spleen and pancreas obviously initiate intense bacterial contamination. Bacterial contamination of pancreatic cells, which was observed later than in the spleen, is also explained by the inhibitory effect of autolytic enzymes of exocrine pancreatic epithelial cells on the intensity of bacterial growth.

The dynamics of destructive post-mortem processes in the cells of internal organs of dog cadavers with different weights and fatness during the experimental period does not significantly differ and develops with the same intensity. However, apart from the direct dynamics of increasing the indicators under study, there is a paradoxical dynamics of cell destruction in the kidneys, pancreas, and brain of dog cadavers and bacterial contamination of the liver and kidneys. In the future, it is planned to continue investigating other cytomorphological characteristics of necroptates of internal organs of dogs in the early post-mortem period in the aspect of forensic veterinary examination.

## References

- [1] Abbate, J.M., Grifò, G., Capparucci, F., Arfuso, F., Savoca, S., Cicero, L., Consolo, G., & Lanteri, G. (2022). Postmortem electrical conductivity changes of *Dicentrarchus labrax* skeletal muscle: Root mean square (RMS) parameter in estimating time since death. *Animals (Basel)*, 2(9), article number 1062. doi: 10.3390/ani12091062.
- [2] Ang, J.Y., Gabbe, B., Cameron, P., & Beck, B. (2019). Animal-vehicle collisions in Victoria, Australia: An under-recognised cause of road traffic crashes. *Emergency Medicine Australasia*, 3(5), 851-855. doi: 10.1111/1742-6723.13361.
- [3] Brooks Brownlie, H.W., & Munro, R. (2016). The veterinary forensic necropsy: A review of procedures and protocols. *Veterinary Pathology*, 53(5), 919-928. doi: 10.1177/0300985816655851.
- [4] Cao, J., Li, W.-J., Wang, Y.-F., An, G.-S., Lu, X.-J., Du, Q.-X., Li, J., & Sun, J.-H. (2021). Estimating postmortem interval using intestinal microbiota diversity based on 16S rRNA high-throughput sequencing technology. *Journal of Forensic Medicine*, 37(5), 621-626. doi: 10.12116/j.issn.1004-5619.2020.400708.

- [5] Ceciliason, A.S., Andersson, M.G., Nyberg, S., & Sandler, H. (2021). Histological quantification of decomposed human livers: A potential aid for estimation of the post-mortem interval? *International Journal of Legal Medicine*, 135(1), 253-267. doi: 10.1007/s00414-020-02467-x.
- [6] Conroy, M., O'Neill, D., Boag, A., Church, D., & Brodbelt, D. (2019). Epidemiology of road traffic accidents in cats attending emergency-care practices in the UK. *Journal of Small Animal Practice*, 60(3), 146-152. doi: 10.1111/jsap.12941.
- [7] Dell'Annunziata, F., Martora, F., Pepa, M.E.D., Folliero, V., Luongo, L., Bocelli, S., Guida, F., Mascolo, P., Campobasso, C.P., Maione, S., & Galdiero, G.F.M. (2022). Postmortem interval assessment by MALDI-TOF mass spectrometry analysis in murine cadavers. *Journal of Applied Microbiology*, 132(1), 707-714. doi: 10.1111/jam.15210.
- [8] Doelling, C.R., Cronin, K.A., Ross, S.R., & Hopper, L.M. (2021). The relationship between personality, season, and wounding receipt in zoo-housed Japanese macaques (*Macaca fuscata*): A multi-institutional study. *American Journal of Primatology*, 83(12), article number 23332. doi: 10.1002/ajp.23332.
- [9] El-Din, E.A.A., Ahmed, S.M., Shafei, D.A.E., & Mostafa, H.E.S. (2021). Implication of high-mobility group box-1 and skin post mortem changes in estimation of time passed since death: Animal and human study. *Legal Medicine*, 53, article number 101949. doi: 10.1016/j.legalmed.2021.101949.
- [10] Franckenberg, S., Kern, F., Vogt, M., Thali, M.J., & Flach, P.M. (2015). Fatal gunshot to a fox: The Virtopsy approach in a forensic veterinary case. *Journal of Forensic Radiology and Imaging*, 3(1), 72-75. doi: 10.1016/j.jofri.2014.11.001.
- [11] Grela, M., Listos, P., Gryzinska, M., Chagowski, W., Buszewicz, G., & Teresinski, G. (2018). Imaging techniques as a method of sectional examination in forensic veterinary medicine. *Veterinary Medicine – Science and Practice*, 12, 751-758. doi: 10.21521/mw.6005.
- [12] Hall, C., Kay, R., & Green, J. (2020). A retrospective survey of factors affecting the risk of incidents and equine injury during non-commercial transportation by road in the United Kingdom. *Animals*, 10(2), article number 288. doi: 10.3390/ani10020288.
- [13] Heng, H.G., Selvarajah, G.T., Lim, H.T., Ong, J.S., Lim, J., & Ooi, J.T. (2009). Serial postmortem abdominal radiographic findings in canine cadavers. *Forensic Science International*, 20, 192(1-3), 43-47. doi: 10.1016/j.forsciint.2009.07.016.
- [14] Kazantsev, R.H., & Yatsenko, I.V. (2021). Cytomorphological changes of a cat's cadaver's parenchymal organs in the early postmortem period in the forensic veterinary examination aspect. *Theoretical and Applied Veterinary Medicine*, 9(3), 146-159. doi: 10.32819/2021.93023.
- [15] Klyuyev, O.M. (2019). Improving the expert development of justice: Theoretical, legal and organizational aspects. *Theory and Practice of Forensic Science and Criminalistics*, 19(1), 102-117. doi: 10.32353/khrife.1.2019.08.
- [16] Law of Ukraine No. 1089-IX "On By-Products of Animal Origin, Not Intended for Human Consumption". (2020, December). Retrieved from <https://zakon.rada.gov.ua/laws/show/287-19#Text>.
- [17] Li, H., Yang, E., Zhang, S., Zhang, J., Yuan, L., Liu, R., Ullah, S., Wang, Q., Mushtaq, N., Shi, Y., An, C., Wang, Z., & Xu, J. (2020). Molecular characterization of gut microbial shift in SD rats after death for 30 days. *Archives of Microbiology*, 202(7), 1763-1773. doi: 10.1007/s00203-020-01889-w.
- [18] Listos, P., Gryzinska, M., Batkowska, J., Dylewska, M., Dudzinska, E., & Piorkowski, J. (2017). Preliminary study on the estimation of the time of death in animals based on microflora development in a canine's gastrocnemius muscle. *Veterinary Medicine – Science and Practice*, 73(4), 229-233. doi: 10.21521/mw.5677.
- [19] Listos, P., Gryzinska, M., Batkowska, J., Dylewska, M., & Czepiel-Mil, K. (2018). Application of research in the field of forensic entomology for determining the time of death in dogs. *Veterinary medicine – Science and Practice*, 74(1), 33-38. doi: 10.21521/mw.5835.
- [20] Listos, P., Gryzinska, M., Piorkowski, J., Teresinski, G., Buszewicz, G., Chagowski, W., Nozdryn-Plotnicki, Z., & Wojciech, L. (2016). Post-mortem estimation of time of death of canines based on measurements of kidney temperature in comparison with rectal temperature. *Acta Veterinaria*, 66(1), 76-88. doi: 10.1515/acve-2016-0006.
- [21] Listos, P., Gryzinska, M., Batkowska, J., Grela, M., & Jakubczak, A. (2018). Algorithm for establishing the time of death of a dog based on temperature measurements in selected sites of the body during the early post-mortem period. *Forensic Science International*, 289, 124-129. doi: 10.1016/j.forsciint.2018.05.004.
- [22] Munro, R., Ressel, L., Gröne, A., Hetzel, U., Jensen, H.E., Paciello, O., & Kipar, A. (2020). European forensic veterinary pathology comes of age. *Journal of Comparative Pathology*, 179, 83-88. doi: 10.1016/j.jcpa.2020.08.003.
- [23] Paltian, J.J., da Fonseca, C.A.R., Pinz, M.P., Luchese, C., & Wilhelm, E.A. (2019). Post-mortem interval estimative through determination of catalase and delta-aminolevulinic acid dehydratase activities in hepatic, renal, skeletal muscle and cerebral tissues of Swiss mice. *Biomarkers*, 24(5), 478-483. doi: 10.1080/1354750X.2019.1619837.
- [24] Panasiuk-Flak, K., Grela, M., & Listos, P. (2021). Determination of the time of death of canines using atropine and pilocarpine in the early post-mortem period – An assessment of the usefulness of the method. *Veterinary Medicine – Science and Practice*, 77(7), 349-352. doi: 10.21521/mw.6546.
- [25] Parry, N.M.A., & Stoll, A. (2020). The rise of veterinary forensics. *Forensic Science International*, 306, article number 110069. doi: 10.1016/j.forsciint.2019.110069.
- [26] Randour, M.L., Smith-Blackmore, M., Blaney, N., DeSousa, D., & Guyony, A-A. (2021). Animal abuse as a type of trauma: Lessons for human and animal service professionals. *Trauma Violence Abuse*, 22(2), 277-288. doi: 10.1177/1524838019843197.
- [27] Ressel, L. (2017). *Normal cell morphology in canine and feline cytology*. Hoboken: Wiley-Blackwell.
- [28] Touroo, R., & Fitch, A. (2016). Identification collection, and preservation of veterinary forensic evidence: On scene and during the postmortem examination. *Veterinary Pathology*, 53(5), 880-887. doi: 10.1177/0300985816641175.

- [29] Welson, N.N., Gaber, S.S., Batiha, G.E.-S., & Ahmed, S.M. (2021). Evaluation of time passed since death by examination of oxidative stress markers, histopathological, and molecular changes of major organs in male albino rats. *International Journal of Legal Medicine*, 135(1), 269-280. doi: 10.1007/s00414-020-02463-1.
- [30] Wunsche, S., Rosati, M., & Matiasek, K. (2016). Diagnostic yield and accuracy of postmortem cytological sampling from the brain surface of animals with neurological abnormalities. *Veterinary Journal*, 211, 57-63. doi: 10.1016/j.tvjl.2016.02.013.
- [31] Yatsenko, I., & Parilovskyi, O. (2020). Recent advances in forensic veterinary examination of animals affected by violent attitude. *Scientific Messenger of LNU of Veterinary Medicine and Biotechnologies. Series: Veterinary Sciences*, 22(97), 95-105. doi: 10.32718/nvlvet9716.
- [32] Yatsenko, I.V., & Kazantsev, R.H. (2021). The procedure of conducting an animal's corpse forensic veterinary examination in the dissecting room of specialized expert institution. *Veterinary Science, Technologies of Animal Husbandry and Nature Management*, 7, 179-191. doi: 10.31890/vttp.2021.07.28.
- [33] Yatsenko, I.V., Parilovsky, O.I., & Kolomoets, D.K. (2019). Issues formation that are used in the court orders and investigator's warrant nominated of forensic veterinary examination of the animal corpse with violent death feature caused by cruelty. *Veterinary Science, Technologies of Animal Husbandry and Nature Management*, 4, 184-197. doi: 10.31890/vttp.2019.04.34.
- [34] Zaporozhan, V.M., Napkhaniuk, V.K., & Horianova, N.O. (2002). *Morphology of blood cells of laboratory animals and humans*. Odesa: Odesa State Medical University.
- [35] Zhang, F.-Y., Wang, L.-L., Zhang, M., Dong, W.-W., Zhang, Z.-D., Li, X.-J., Ma, X.-Y., Du, S.-K., Yuan, H.-M., Guan, D.-W., & Zhao, R. (2022). Inferring postmortem submersion interval in rats found in water based on vitreous humor metabolites. *Journal of Forensic Medicine*, 38(1), 59-66. doi: 10.12116/j.issn.1004-5619.2021.410613.

## Цитоморфологічна характеристика некроптів внутрішніх органів собак у ранньому постмортальному періоді в аспекті судово-ветеринарної експертизи

Іван Володимирович Яценко<sup>1</sup>, Роман Геннадійович Казанцев<sup>2</sup>

<sup>1</sup>Доктор ветеринарних наук, професор. ORCID: <https://orcid.org/0000-0001-8903-2129>.

Інститут ветеринарної медицини та тваринництва,  
62341, вул. Академічна, 1, сел. Мала Данилівка, Харківська область, Україна

<sup>2</sup>Аспірант. ORCID: <https://orcid.org/0000-0002-4479-1516>.

Інститут ветеринарної медицини та тваринництва,  
62341, вул. Академічна, 1, сел. Мала Данилівка, Харківська область, Україна

**Анотація.** Актуальність дослідження зумовлена потребою судово-ветеринарної експертизи трупів тварин щодо наукового обґрунтування інформативних діагностичних критеріїв для оцінки давності настання смерті, особливо у ранньому постмортальному періоді. Проте, інформація щодо ранніх постмортальних змін трупів собак на мікроструктурному рівні в українській та зарубіжній науковій літературі має досить фрагментарний характер. У зв'язку з цим дана стаття спрямована на з'ясування інформативності динаміки процесів клітинної деструкції та бактеріальної контамінації внутрішніх органів трупів собак упродовж першої постмортальної доби для встановлення вірогідних експертних критеріїв давності настання смерті підекспертних тварин під час проведення судово-ветеринарної експертизи. Провідним підходом до дослідження цієї проблеми є методи отримання від трупів собак серії некроптів із легенів, серця, печінки, селезінки, нирок, підшлункової залози та головного мозку, через однаковий часовий інтервал упродовж першої доби після настання смерті. У цитологічних препаратах, отриманих з некроптів, підраховували кількість зруйнованих клітин і бактеріальних одиниць за допомогою оптичної мікроскопії. За результатами динаміки бактеріальної контамінації та інтенсивності морфологічних змін клітин селезінки та підшлункової залози встановлена їхня експертна інформативність щодо вирішення питання про давність настання смерті собак, незалежно від показників ваги та вгодованості. З'ясовано, що динаміка бактеріальної контамінації і клітинної деструкції головного мозку, нирок і легенів трупів собак мають середню експертну інформативність, а печінки та серця – не інформативні. Доведено, що динаміка руйнівних післясмертних процесів у клітинах компактних органів трупів собак різної маси та вгодованості на відповідних термінах вірогідно не відрізняються та розвиваються з однаковою інтенсивністю. Отримані результати дослідження матимуть значення як у теорії судово-ветеринарної експертизи, так і безпосередньо прикладне, зокрема, під час вирішення судовим експертом питання щодо давності настання смерті тварини

**Ключові слова:** підекспертні тварини, трупна біотрансформація, клітинна деструкція, бактеріальна контамінація, посмертні зміни органів